APPLICATIONS OF THE ADVANCED SIMULATION CAPABILITY FOR ENVIRONMENTAL MANAGEMENT (ASCEM)-17253

Mark Freshley*, David Moulton**, Haruko Wainwright***, Sergi Molins***, Kay Birdsell**, Dylan Harp**, Zhiming Lu**, Edward Kwicklis**, Velimir Vesselinov**, Daniel O'Malley**, Danny Katzman**, Konstantin Lipnikov**, Vicky Freedman*, Erin Barker*, and Paul Dixon**
*Pacific Northwest National Laboratory, MSIN K9-33, P.O. Box 999, Richland, WA 99352
**Los Alamos National Laboratory, MS B284, P.O. Box 1663, Los Alamos, NM 87544
***Lawrence Berkeley National Laboratory, 1 Cyclotron Road, MS 50B-4230, Berkeley, CA 94720

Three applications were completed using the Advanced Simulation Capability for Environmental Management (ASCEM), supported by the U.S. Department of Energy's Office of Environmental Management. These analyses were performed for the Savannah River Site (SRS) F-Area, the Los Alamos National Laboratory (LANL) Site, and the Nevada National Security Site (NNSS). At the SRS F-Area, ASCEM simulations were used to help develop cost-effective, long-term monitoring approaches for science-based site closure and management. The simulation results were used to develop a mechanistic understanding of correlations between contaminant concentrations and master variables that can be used for monitoring. At LANL, the ASCEM simulator Amanzi was integrated with a LANL-based decision support tool for the LANL onsite program. A saturated-zone site model focused on a key area of interest was developed and calibrated to measured data. This model was applied to quantify uncertainty and provide decision support to inform chromium remediation efforts. To support assessment of groundwater contamination at NNSS, ASCEM was used to calibrate hydrologic properties and flow directions using water levels observed under steady-state conditions and during four different pump tests on Pahute Mesa. The flow fields generated from these pump tests will be used to simulate transport pathways from underground nuclear tests to compare with field observations and to test alternative conceptual models of transport, which will ultimately facilitate better placement of monitoring wells.

INTRODUCTION

The Office of Soil and Groundwater Remediation within the U.S. Department of Energy Office of Environmental Management (EM) developed the Advanced Simulation Capability for Environmental Management (ASCEM). ASCEM is a collection of toolsets that provides 1) a workflow [1] consisting of a set of pre- and post-processing tools for translating conceptual models into numerical models; and 2) a reactive flow and transport simulator for predicting contaminant fate and transport in the subsurface. This workflow is based on a client-server architecture that allows users access to high-performance computing resources. Multiple toolsets are available, including model setup, calibration, sensitivity analysis, and uncertainty quantification; both risk and decision support toolsets are being

developed. ASCEM promotes collaborative modeling through file access for multiple users on a shared server.

ASCEM is an open source software infrastructure for understanding and predicting contaminant fate and transport in natural and engineered subsurface systems. ASCEM facilitates integrated approaches that enable standardized assessments of performance and risk for EM cleanup and closure decisions. The ASCEM project is using a phased deployment approach, starting with site applications that were used to guide software development, and currently with initial deployments to provide technical underpinnings for performance assessments. The deployments include the Savannah River Site (SRS) F-Area, the Los Alamos National Laboratory (LANL) Site, and the Nevada National Security Site (NNSS).

URANIUM PLUME MIGRATION AT THE SAVANNAH RIVER SITE F-AREA

This section demonstrates both ASCEM's reactive transport capabilities as well as the uncertainty quantification toolset. The SRS F-Area application consisted of an integrated flow-geochemistry-transport model. ASCEM's advanced simulation capabilities enabled a systems-based approach that integrates laboratory and field measurements with modeling for long-term management of remediation and monitoring of metals and radionuclides. The model was also applied to explore a new approach for long-term monitoring based on continuous in situ monitoring of geochemical master variables that control plume mobility, such as pH, electrical conductivity, and water table. ASCEM (1) provided mechanistic and predictive understanding of contaminant plume mobility and behavior, and (2) were used to evaluate the sensitivity and effectiveness of new monitoring approaches.

ASCEM has been applied to evaluate the effects of past and current engineering systems on flow and the geochemical conditions of the site, and to predict the time frame for transition from active remediation to monitored natural attenuation. A three-dimensional flow and reactive transport model of the SRS F-Area was developed and modified in 2015 to describe the impact of engineered systems and complex geochemical conditions at the site. ASCEM was applied to compute the uncertainty range of predictions for robust decision-making. The model was also used to assess the efficacy of the long-term monitoring strategies through advanced visualization and modeling. The model was used to estimate the plume extent, determine the optimal layout of a monitoring network, and understand the effect of master variables on contaminant mobility.

The three-dimensional hydrological model is based on a previous flow model developed for a larger domain encompassing the overall General Separations Area (GSA) at SRS [2]. The flow velocity field computed in the GSA flow model was used to define a model domain that follows natural hydrogeologic boundaries (Fig. 1). The hydrostratigraphic units were updated based on recently collected cone penetrometer testing data and surface seismic data [3], including a clay confining layer that is known to affect uranium transport. In addition, the new model includes low-permeability engineered barriers, which were constructed part of the funnel-and-gate system in 2004.

The final mesh used in this study has 1,849,039 cells and 982,998 vertices, representing an order of magnitude greater refinement than the previous model of the GSA [2]. The increased mesh refinement allowed realistic representation of boundary conditions and engineered features in the model.

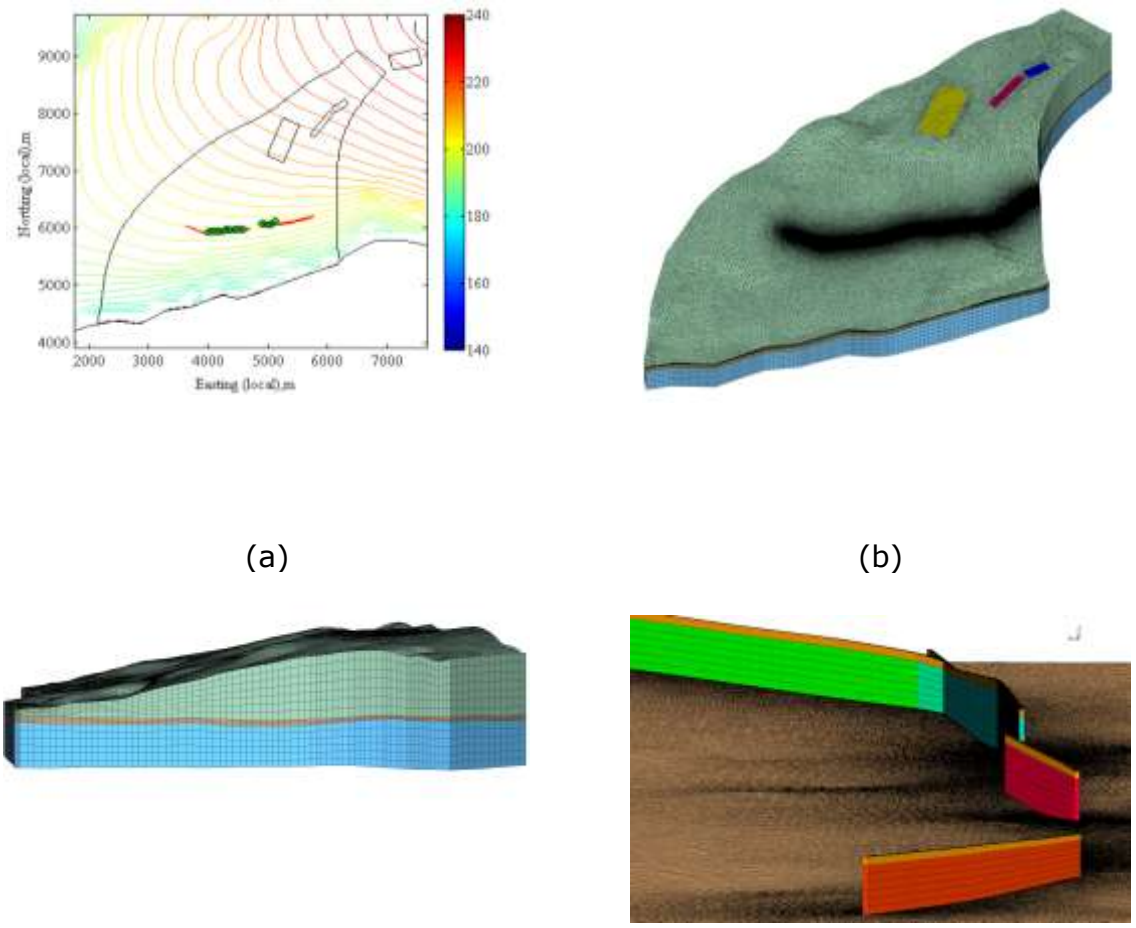

Fig. 1. (a) Plan view of the model domain; (b) three-dimensional mesh including three hydrostratigraphic units, the F-Basin site (yellow), and each of the three barriers (red); (c) a cross-section view of the mesh; and (d) a cutaway of the mesh showing the barriers (red, blue, and green) and the Tan Clay interface (brown). In (b) and (c), the top green material region is the upper aquifer, the middle brown layer is the Tan Clay confining zone, and the bottom blue region is the lower aquifer.

Fig. 2 shows the simulated evolution of the low-pH and uranium plumes. This simulation includes capping of the seepage basin, which limited the infiltration after the basin operation stopped. It does not include other remediation treatments at the site. The plumes initially move straight down vertically until they hit the water table, and then migrate laterally, mainly within the upper aquifer (Fig. 2a and d).

The low-pH plume moves more quickly down gradient (Fig. 2a and b), increasing the mobility of uranium and creating a way for the uranium plume to follow (Fig. 2d and e). As the plume migrates down gradient towards the creek, the plume goes through the troughs in the bottom of the upper aquifer (Fig. 2b). The model predicts that a significant amount of uranium will be trapped in the vadose zone (Fig. 2f) in 2050, even though pH is neutralized (Fig. 2c), which suggests the long-term effect of capping the basin. The model shows strong correlations between predicted uranium concentrations and pH over time, particularly in the trailing edge of the plume. Additional detail regarding the simulations and results can be found in Wainwright et al. [3].

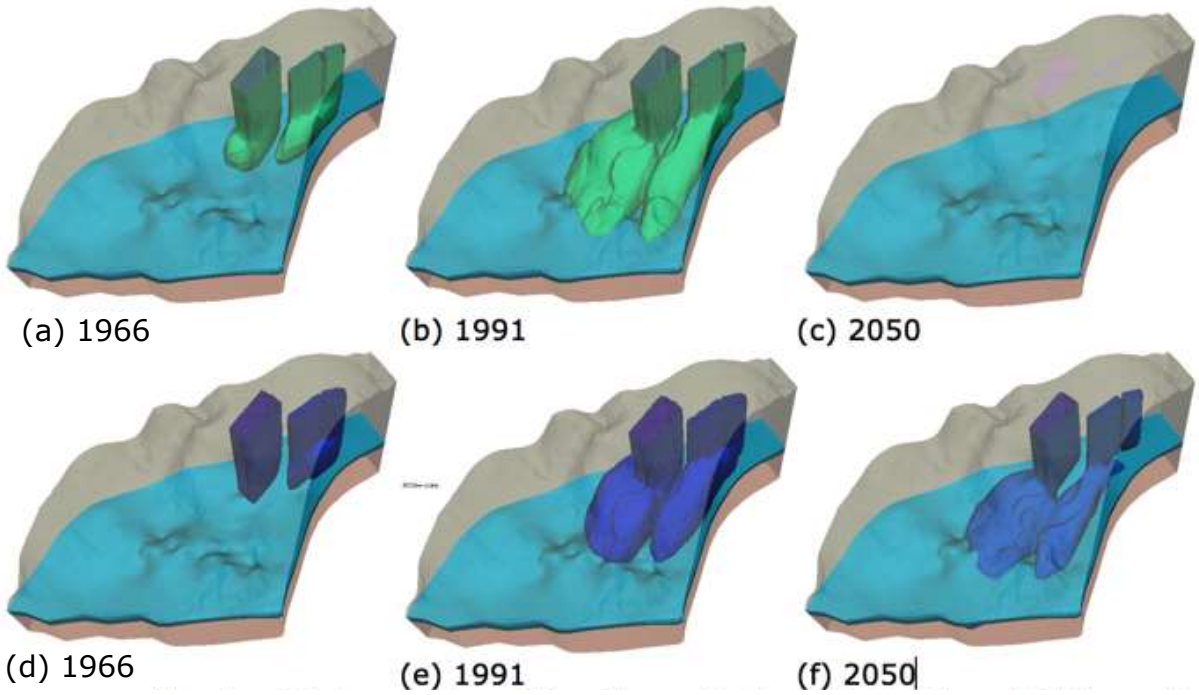

Fig. 2. The simulated evolution of a low-pH plume (pH> 4) at 1966 (a), 1991 (b), and 2050 (c) and a uranium plume (concentration>$1x10^{-6}$mol/L) at 1966 (d), 1991 (b), and 2050 (c). The sky blue region is a low permeable region, which separates the upper and lower aquifers. Vertical exaggeration=15X.

LANL SITE CHROMIUM

This section demonstrates how decision support tools can be used to inform remediation efforts. The chromium plume at LANL poses a complex challenge for remediation because of the complex migration pathway and the depth of the target groundwater zone. The plume footprint covers several square kilometers within a deep aquifer (~300 m) and is located near water-supply wells and the LANL Site boundary. The contamination originated from cooling tower blowdown and migrated along complex pathways through a thick vadose zone that includes intermediate-depth perched zones of saturation and vertical preferential flow paths. Typical remedial alternatives are being evaluated, including natural attenuation,

contaminant extraction from the plume center, enhanced in situ remediation using bio and/or chemical amendments, and hydraulic controls on the groundwater flow and transport in the vadose zone and the regional aquifer.

The LANL site has actively applied a computational framework to address chromium contamination [4,5,6]. Data and model analyses are performed using the Model Analysis and Decision Support (MADS) framework [7]. MADS is a high-performance, open-source framework for model-based decision support, including efficient optimization of large inverse problems, sensitivity analyses, uncertainty quantification, decision analyses, and experimental design [8,9,10,11,12].

In this effort, MADS was coupled with ASCEM's Amanzi simulator. Amanzi provides several critical capabilities for EM modeling work at the chromium site. First, it supports advanced discretizations that remain accurate in the presence of grid distortions and pinch-outs, and which are not available in other currently deployed codes. In addition, these discretizations accurately capture the stratigraphic layers present in the geologic framework model, without smearing the location of the interfaces. These factors help to ensure that the simulated flow field that drives the transport of contaminants is accurately captured, even at geologically complex sites. A second important benefit of these advanced discretizations is that they enable Amanzi to accurately capture non-grid-aligned dispersion, which is critical in the analysis and prediction of plume migration and plume response to various remedial actions. This capability is highlighted in Fig. 3, where a snapshot of a plume resulting from saturated flow at 45 degrees (lower left to upper right) with isotropic dispersion is shown for a flow-aligned (a) and non-flow-aligned grid (b and c). The plumes are superimposed on the underlying computational mesh, which was rotated 45 degrees in the non-grid-aligned case. Since the underlying physics model is the same in all cases, the plume should be the same in all cases, and the differences are entirely an artifact of the discretization process. It is apparent in these figures that only small differences in the plume result from two different grids in the case of the advanced discretization, while significant differences in the plume result from the standard discretization. These differences can significantly affect the design and cost of remediation and monitoring strategies.

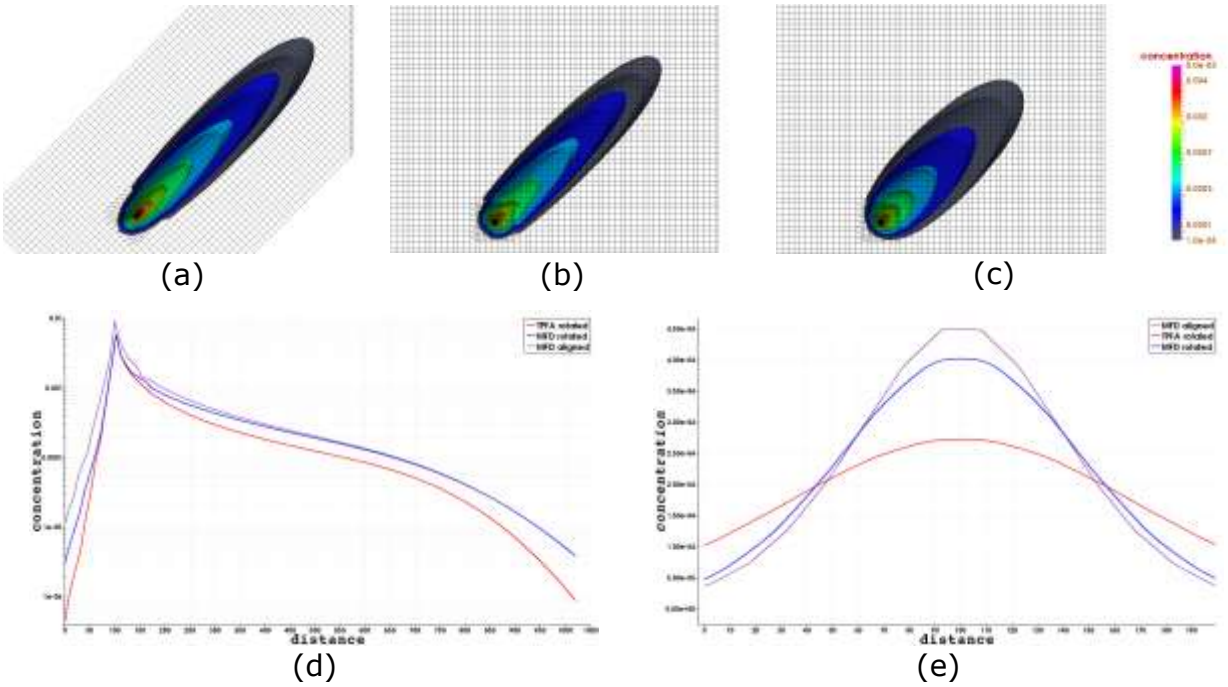

Fig. 3. A non-reactive tracer that is dispersed from a point source by a saturated flow at 45 degrees (lower left to upper right) is simulated with Amanzi using a flow-aligned grid and a non-flow-aligned grid. Isosurfaces of the plume, cut by the top surface of the domain, are shown in the top row of images (a-c). With the flow-aligned grid (a), dispersion is naturally grid-aligned and both the standard discretization (TPFA) and the advanced discretization (MFD) produce consistent and accurate results. With the non-flow-aligned grid, the MFD method (b) remains accurate, while the TPFA method (c) exhibits significant grid effects. These effects are shown more quantitatively in the centerline cross-section (d), where the TPFA simulated plume moves more slowly, and in the transverse cross-section (e), where the TPFA simulated plume is dispersing laterally much more quickly than the MFD simulated plume.

To support evaluation of the chromium plume and interface with MADS, several enhancements were made to Amanzi. First, the input specification was enhanced to make it easier to define chromium-related base problems, as well as the related ensemble of simulations. For example, to ease the use of site data, the ability to explicitly control units was significantly improved, and support for input and output concentrations in ppb and ppm was added. Second, the flexible and powerful mesh infrastructure in Amanzi enabled the efficient development of non-grid-aligned contaminant source regions that use volume fractions to improve the performance of the inversion algorithms used in MADS for estimating source properties (spatial distribution, contaminant concentration, etc.) from simulated plume evolution. Similarly, an alternative workflow for supporting heterogeneous fields was developed, significantly reducing the model setup time required during an ensemble of runs on a given computational grid within MADS.

To build confidence in Amanzi for application to the chromium problem, it was benchmarked with an existing simulator, Finite Element Heat and Mass (FEHM). First, a set of flow problems was set up on a simplified model of the site using real locations for pumping wells. Then several multi-well scenarios were tested to demonstrate agreement between Amanzi and FEHM. For example, Fig. 4 shows simulated heads at selected observation points. Fig. 5 presents simulated breakthrough curves for the case of uniform steady-state groundwater flow field. The presented results show a good match between Amanzi and FEHM predictions.

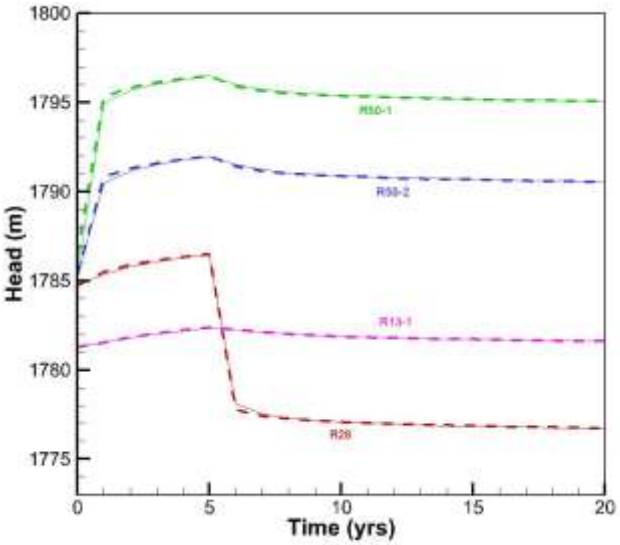

Fig. 4. Simulated heads using FEHM (solid lines) and Amanzi (dashed lines) at selected monitoring wells.

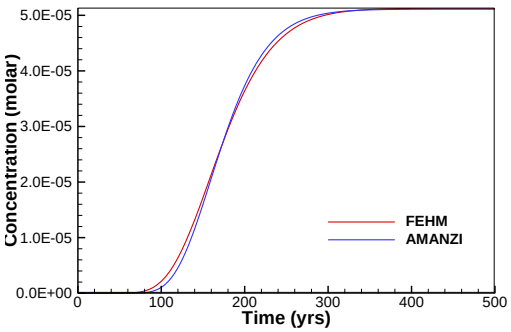

Fig. 5. FEHM- and Amanzi-computed breakthrough curves for the case of uniform steady-state groundwater flow field.

To execute a coupled simulation, MADS creates an Amanzi input file for a given set of input model parameters to execute Amanzi. After Amanzi execution is completed, MADS processes the Amanzi output files to obtain information about how the changes in the input model parameters affect the obtained model predictions. The

model-predicted observations are applied to perform model-based analyzes of model parameters using MADS. The analyzed model parameters are related to (1) groundwater flow boundary conditions, (2) contaminant transport boundary conditions, and (3) aquifer properties. MADS and Amanzi have been applied to perform model calibration and sensitivity analyses (local and global). MADS also provides additional tools to visualize and analyze the obtained results. Fig. 6 shows a global sensitivity analysis performed using MADS and Amanzi for a set of model parameters related to model-predicted concentrations at the monitoring wells. Fig. 6 shows the total effect sensitivity indices for the explored model parameters at one of the site monitoring wells (R-28) to model boundary conditions parameters. The analysis required 385 forward model runs that were completed in parallel using high-performance computing.

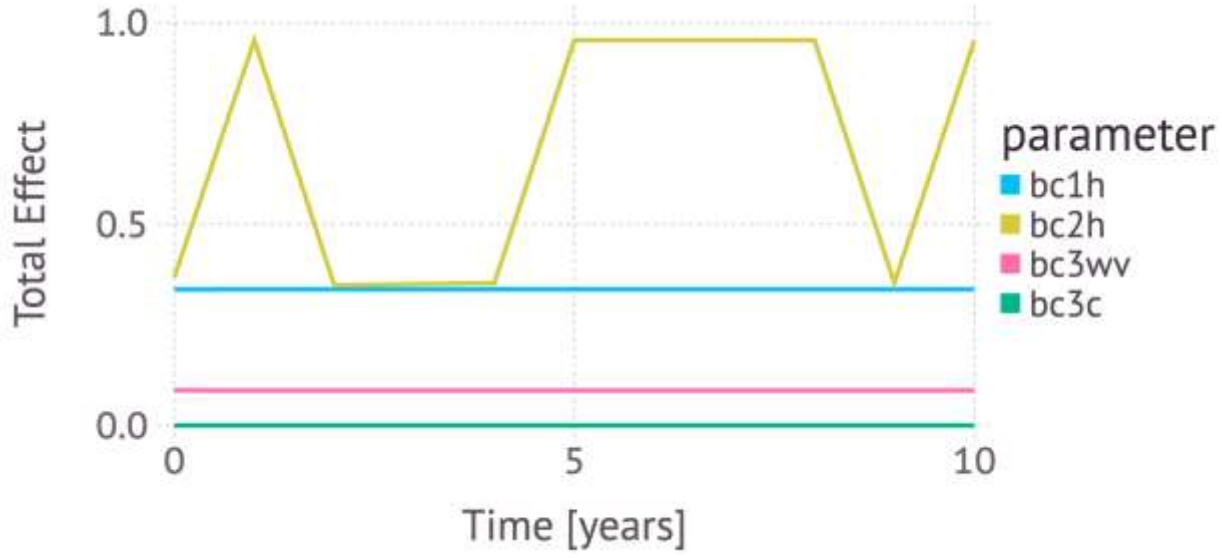

Fig. 6. Total effect sensitivity over time at a monitoring well; the total effect indices are estimated relative to uncertain model boundary conditions using MADS coupled with Amanzi (bc1h = upgradient constant head boundary condition, bc2h = downgradient constant head boundary condition, bc3wv = source water flux, bc3c = source concentration).

NNSS GROUNDWATER ASSESSMENT

This section demonstrates the coupling of Amanzi and parameter estimation tools for model calibration. The Amanzi flow simulator was used to support assessment of groundwater flow at the NNSS. Amanzi was driven by parameter estimation software [13] to calibrate hydrologic properties and flow directions for a large domain covering much of Pahute Mesa, where 85 deep underground nuclear tests were conducted. Fig. 7 shows the hydrologic framework model within the 20- by 35- by 2.5-km simulation domain. The numerical mesh has 7.06 million cells, and the domain consists of 51 different geologic units and 44 major faults. The grid

resolution was 100 by 100 m in the horizontal direction and 25 m in the vertical direction.

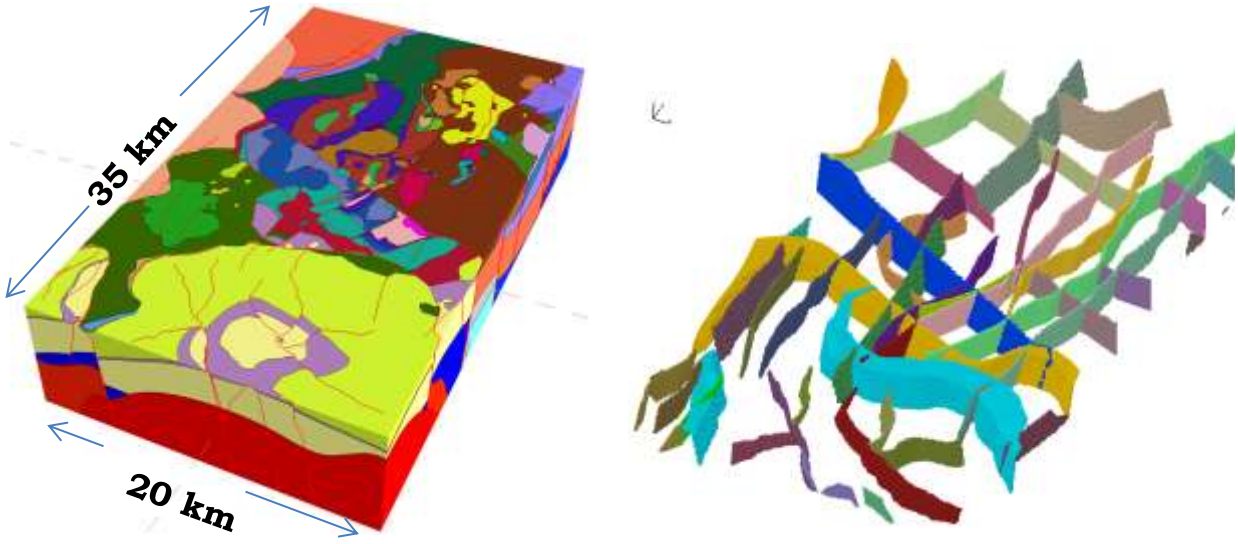

(a) (b)

Fig. 7. Geologic model and domain (a), and fault distribution (b) used by the NNSS applications domain

Model calibration used water levels observed under both steady-state conditions and during four different pump tests on Pahute Mesa. The calibration simultaneously inverted data for steady-state heads at 70 locations, and 2200 transient drawdown measurements from 32 well screens observed over a 6-year period. A total of 190 model parameters were estimated: 95 permeability and 95 specific storage coefficients for the different geologic units and faults.

The simulation results compare well to both the steady-state and transient water levels. Model residuals were efficiently reduced using super parameters in the parameter estimation software. Fig. 8 compares the contours of the measured steady-state heads to those from the calibrated model. Fig. 9 shows an example of transient drawdown data for three well screens compared with simulation results at an observation well in the model domain.

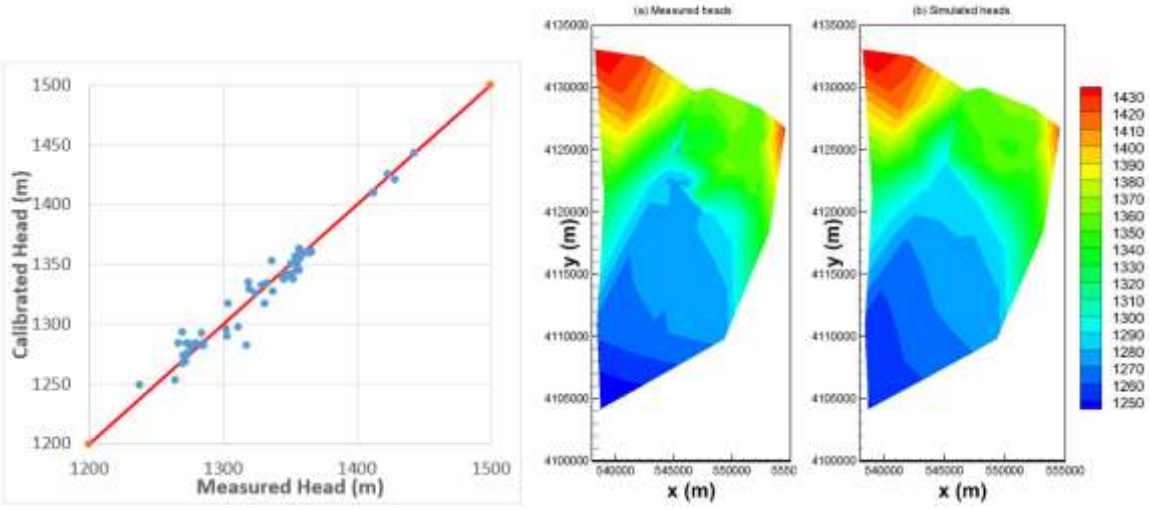

Fig. 8. Comparison of steady-state measured and calibrated head data.

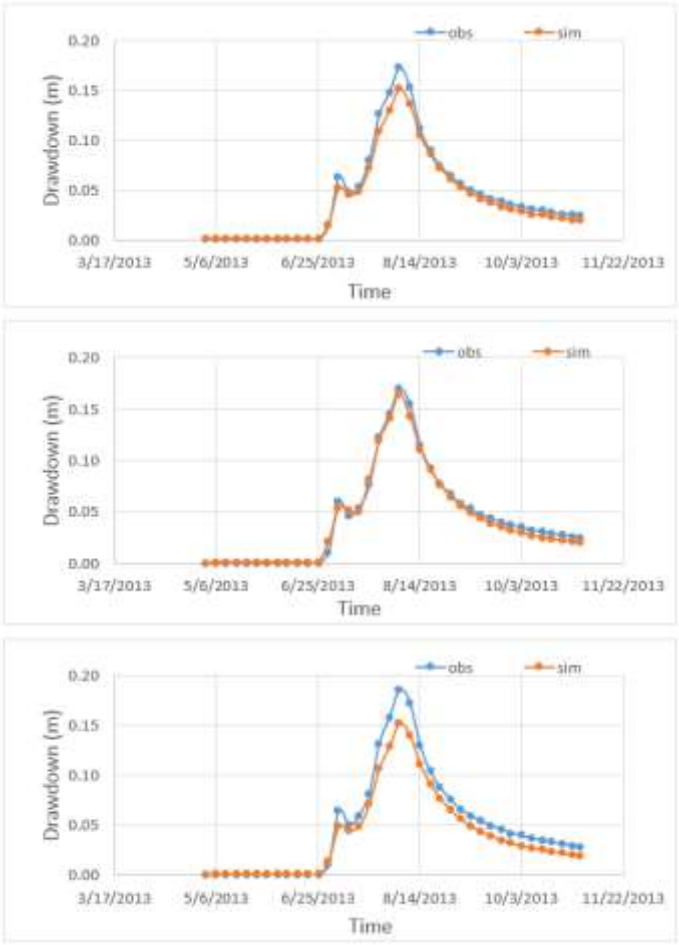

Fig. 9. Comparison of transient drawdown data and simulation results for three well screens (shallow, intermediate, deep) in observation well ER-20-8 in response to pumping at well ER-20-11.

The flow model calibration was run on a high-performance computing Linux cluster at LANL. To accelerate the initialization of each forward run, the mesh was pre-partitioned into 480 subdomains. One forward run of the flow simulation used 480 cores and took approximately 15 to 20 minutes. During calibration, six forward runs were run concurrently on 2896 cores to optimize 60 parameters.

CONCLUSIONS

The applications described in this paper are intended to highlight ASCEM capabilities for evaluation of remediation strategies and performance assessments over baseline capabilities. Development of ASCEM has matured to the point where it was applied to address specific issues facing DOE sites.

Modeling is a tool that can be used to make informed choices in uncertain and complex environments, where costs and benefits of environmental impacts and human health need to be considered. Various tools that have been integrated with Amanzi provide analysis capabilities needed for decision-making at DOE sites. Parameter estimation for model calibration, uncertainty analysis and decision support toolsets are capabilities critical to this effort. These toolsets are being incorporated into a unified framework to extend simulation capabilities, facilitate efficient modeling and analyses, and address costs and benefits of decisions made at waste sites. This efficiency, and the ease of access to analysis methods, maximizes available information to address and mitigate sources of uncertainty in subsurface analyses.

The analysis of the SRS F-Area included detailed simulations using a three-dimensional unstructured mesh that accounted for fine-scale discretization to represent the engineered barriers, seepage basin, and injection/extraction wells. Increased mesh refinement allowed realistic representation of boundary conditions and engineered features in the model. Simulation of the system included changes over time for capping the seepage basin and placement of the low-permeability barriers in 2004, a significant improvement in modeling dynamic changes of engineered systems. Access to high-performance computing resources enabled a more refined mesh and model complexity to be simulated. A two-dimensional model was used to correlate between master variables (pH, water table elevation, and electrical conductivity) and contaminant concentrations. These results confirm the effectiveness and robustness of a new approach for long-term monitoring using master variables, although they need to be compared with the three-dimensional reactive transport model.

To support the modeling needs at the Chromium site, including the analyses optimizing decision goals related to placement of new wells, monitoring frequencies, and remedial strategies, Amanzi capabilities were enhanced. These enhancements included improvements to the input specification and controls, managing volume fractions for non-grid-aligned sources, and improving workflow for heterogeneous materials. A suite of benchmarking tests was run to ensure that the existing core capabilities of Amanzi, and its new enhancements, are performing correctly. This began with flow tests with multiple wells, and then considered transport tests with

multiple sources. In all cases, good agreement with FEHM code was obtained. The MADS capabilities for working with external simulators were further enhanced as well to accommodate the needs and requirements of Amanzi. Finally, a model-analysis of the chromium site model was performed by MADS coupling with Amanzi. These successes position the team to further advance the complexity of the model and conduct advanced model-based decision analyses for this hydrogeologically complex site.

The Amanzi calibration for the NNSS application using high performance computing proved to be a very successful demonstration of ASCEM capabilities. This application provided a computationally-efficient representation of the complex NNSS geologic setting composed of fractured and faulted volcanic aquifers using a high-resolution 7-million node mesh, and simultaneous inversion of steady-state and transient data. The ability to solve such a complex problem is not available with other simulation platforms. Now that we have this high-fidelity flow field, further use of ASCEM tools for the NNSS will examine alternative conceptual models of radionuclide transport from testing areas at the site.

REFERENCES

1. FREEDMAN, V. L., CHEN, X., FINSTERLE, S. A., FRESHLEY, M. D., GORTON, I., GOSINK, L. J., KEATING, E., LANSING, C., MOEGLEIN, W. A. M., MURRAY, C. J. PAU, G. S. H., PORTER, E. A., PUROHIT, S., ROCKHOLD, M. L., SCHUCHARDT, K. L., SIVARAMAKRISHNAN, C., VESSELINOV, V. V., and WAICHLER, S. R. "A high-performance workflow system for subsurface simulation." *Environmental Modelling & Software* 55,176-189 (2014). doi:10.1016/j.envsoft.2014.01.030
2. FLACH, G. *Groundwater Flow Model of the General Separations Area Using Porflow (U).* WSRC-TR-2004-00106, Westinghouse Savannah River Company, Aiken, SC (2004).
3. WAINWRIGHT, H. M., MOLINS, S., DAVIS, J. A., ARORA, B., FAYBISHENKO, B., KRISHNAN, H., HUBBARD, S., FLACH, G., DENHAM M., EDDY-DILEK, C., MOULTON, J. D., LIPNIKOV, K., GABLE, C., MILLER, T., and FRESHLEY, M. "Using ASCEM Modeling and Visualization to Inform Stakeholders of Contaminant Plume Evolution and Remediation Efficacy at F-Basin Savannah River, SC." In *Waste Management Symposia*, Phoenix, AZ, USA, March 15-19 (2015).
4. VESSELINOV, V., MALLEY, D. O., and KATZMAN, D. "Model-Assisted Decision Analyses Related to a Chromium Plume at Los Alamos National Laboratory," *Waste Management Symposia*, Phoenix, AZ, USA, March 15-19 (2015).
5. VESSELINOV, V. V., BROXTON, D., BIRDSELL, K., RENEAU, S., HARP, D. R., MISHRA, P. K., and JACOBS, E. "Data and Model-Driven Decision Support for Environmental Management of a Chromium Plume at Los Alamos National Laboratory." In *Waste Management Symposia*. Phoenix, AZ, USA (2013).
6. VESSELINOV, V. V., O'MALLEY, D., and KATZMAN, D. "ZEM: Integrated Framework for Real-Time Data and Model Analyses for Robust Environmental Management Decision Making." In *Waste Management Symposia*. Phoenix, AZ, USA, (2016).

7. VESSELINOV, V. V., and O'MALLEY, D. "Model Analysis of Complex Systems Behavior using MADS." In *Proceedings American Geophysical Union Fall Meeting,* San Francisco, CA (2016).
8. HARP, D. R., and VESSELINOV, V. V. "An agent-based approach to global uncertainty and sensitivity analysis." *Computers & Geosciences* 40,19–27 (2012). http://doi.org/10.1016/j.cageo.2011.06.025
9. MATTIS, S. A., BUTLER, T. D., DAWSON, C. N., ESTEP, D., and VESSELINOV, V. V. "Parameter estimation and prediction for groundwater contamination based on measure theory." *Water Resources Research* 51(9) (2015). http://doi.org/10.1002/2015WR017295
10. O'MALLEY, D., and VESSELINOV, V. "A Combined Probabilistic/Nonprobabilistic Decision Analysis for Contaminant Remediation." *SIAM/ASA Journal on Uncertainty Quantification 2*(1), 607–621 (2014a). http://doi.org/10.1137/140965132
11. O'MALLEY, D., and VESSELINOV, V. V. "Groundwater remediation using the information gap decision theory." *Water Resources Research* 50(1), 246–256 (2014b). http://doi.org/10.1002/2013WR014718
12. VESSELINOV, V. V., and HARP, D. R. "Adaptive hybrid optimization strategy for calibration and parameter estimation of physical process models." *Computers & Geosciences*, 49(98), 10–20 (2012). http://doi.org/10.1016/j.cageo.2012.05.027
13. DOHERTY, J. *Calibration and Uncertainty Analysis for Complex Environmental Models*. Watermark Numerical Computing, Brisbane, Australia. ISBN: 978-0-9943786-0-6 (2015).

ACKNOWLEDGEMENT

This work was supported with funding provided by the Office of Soil and Groundwater Remediation within the U.S. Department of Energy's Office of Environmental Management. Approved for public release by the NNSA/NFO Technical Information Review Program under Log No. 2016-195.